INSTITUTE OF PHYSICS PUBLISHING JOURNAL OF PHYSICS: CONDENSED MATTER

J. Phys.: Condens. Matter **14** (2002) 2193–2200 PII: S0953-8984(02)32440-8

Liquid–liquid phase transition in one-component fluids

Gianpietro Malescio[1], Giancarlo Franzese[2], Giuseppe Pellicane[1], Anna Skibinsky[2], Sergey V Buldyrev[2] and H Eugene Stanley[2]

[1] Dipartimento di Fisica, Università di Messina and Istituto Nazionale Fisica della Materia, 98166 Messina, Italy
[2] Center for Polymer Studies and Department of Physics, Boston University, Boston, MA 02215, USA

Received 8 January 2002
Published 22 February 2002
Online at stacks.iop.org/JPhysCM/14/2193

Abstract

The stability of a one-component model system interacting through an isotropic potential with an attractive part and a softened core is investigated through integral equations and molecular dynamics simulation. The 'penetrability' of the soft core makes it possible for the system to pass from an expanded liquid structure at intermediate densities to a more compact one at high densities.

When speaking of liquid–liquid transitions, one usually thinks of multi-component systems such as fluid mixtures. In fact, as is well known, these systems are not always miscible and may separate into two fluids with different concentrations and densities. In the last few years the possibility that single-component systems may also exhibit a liquid–liquid transition has received considerable attention. Recent experimental results [1] indicate that phosphorus can have a high-density-liquid (HDL) and a low-density-liquid (LDL) phase. A first-order transition between two liquids of different densities [2] is consistent with experimental data for a variety of materials including single-component systems such as water [3–6], silica [7] and carbon [8]. Moreover, molecular dynamics (MD) simulations of specific models for supercooled water [2, 9], liquid carbon [10] and supercooled silica [11] predict a LDL–HDL critical point.

Several explanations have been developed to explain the liquid–liquid phase transition, based on the use of anisotropic potentials [2, 9–11] or on two-liquid models [12]. Recently [13, 14] it was shown through numerical simulation and theoretical approaches that the presence of a LDL and a HDL can arise solely from an isotropic interaction potential with an attractive part and with *two* characteristic short-range repulsive distances.

In molecular liquid phosphorus as well as in water, expanded and compact structures compete with each other and are preferred respectively at low and high pressures and temperatures [1, 4, 6]. This suggests a pair interaction with two characteristic distances. The first distance can be associated with the *hard-core* exclusion between two particles and the second distance with a weak (*soft-core*) repulsion which can be overcome at large pressure.

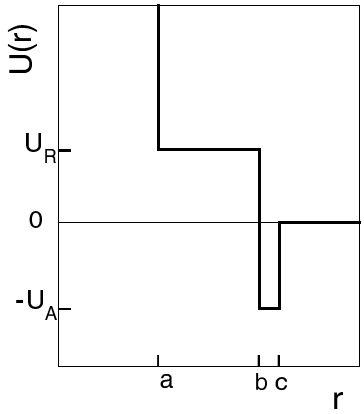

Figure 1. The pair potential $U(r)$ as a function of the distance r between two particles.

These features can be incorporated into a simple isotropic soft-core pair potential to be regarded as resulting from averaging over the angular parts of more realistic potentials. An isotropic potential with a softened core has already been proposed in the literature in several different contexts including those of simple metals [2, 15–17] and supercooled liquids [18–20].

The isotropic pair potential considered here (figure 1) consists of a hard core of radius a with a repulsive square shoulder of height $U_R > 0$ and radius $b > a$, plus an attractive component having the form of a square well of depth $-U_A < 0$ extending from $r = b$ to $r = c$. If we choose the hard-core radius as the length unit and the well depth as the unit of energy, we are left with three free parameters: b/a, c/a and U_R/U_A. Since the number of possible combinations of these is huge it is useful to perform a first qualitative analysis of the phase behaviour of the system using a fast, even if not very accurate, investigation method.

Integral equations for the radial distribution function [21] may provide such a tool. One of the simplest integral theories is the hypernetted-chain (HNC) equation [21]. For such an equation there exists a region of ρ–T thermodynamic plane where no solution can be found. A strict identification of the locus of the points below which the theory ceases to work with the spinodal line of the fluid is not possible. In fact, though the isothermal compressibility considerably increases when this region is approached from above, a real divergence of the isothermal compressibility is predicted by the theory only in some particular density–temperature regimes [22]. In spite of this limitation, it has been observed that, for a large number of simple fluid pair potentials, the shape of the region where no solution is found qualitatively resembles the region of spinodal decomposition of the fluid, where the system separates into two fluid phases [23].

Due to its approximate nature, the HNC equation is thermodynamically inconsistent, i.e. the equations of state obtained following the virial, compressibility and energy routes do not coincide. There are a number of ways [23] in which this inconsistency can be removed, giving rise to more reliable theories. So it is possible to obtain more accurate estimates of the spinodal line and, being the new theory thermodynamically consistent, also to calculate the binodal line. However, due to the additional numerical procedures needed to impose the thermodynamical consistency requirement, these equations, though much faster than numerical simulation, needs more computational time than the HNC equation, which thus appears well suited for an extensive investigation in the parameter space of the model potential.

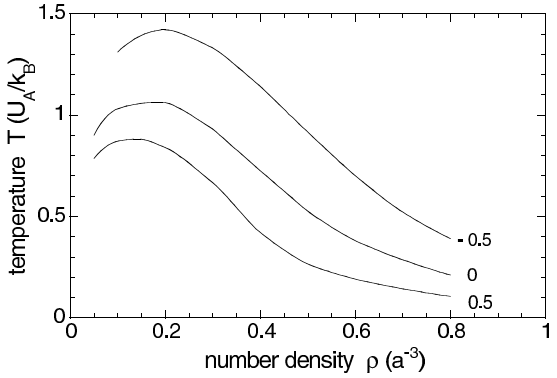

Figure 2. The instability line of the HNC equation ($b/a = 1.4, c/a = 1.7$). Each curve is labelled with the corresponding value of U_R/U_A.

We first calculate the instability line of the HNC equation for the potential investigated in [19]. The corresponding parameters are $b/a = 1.4$, $c/a = 1.7$, $U_R/U_A = -0.5$. In this case the repulsive shoulder is, so to say, 'buried' in the attractive well. Though it was shown that the system shows thermodynamic anomalies typical of water [19], the instability line of the HNC equation (see figure 2) is similar to the spinodal line usually exhibited by a simple fluid, such as a Lennard-Jones fluid. Upon increasing the height of the shoulder there is no evident topological change of the line (even for positive values of U_R/U_A), other than a shift towards lower temperatures as a result of the overall decrease of the interparticle attraction.

We next consider a potential with a shoulder wider than that of the previous case and an attractive well having the same width ($b/a = 1.7, c/a = 2$). The instability line was calculated for several values of U_R/U_A (see figure 3). We found that upon increasing the height of the shoulder the maximum of the line moves markedly to lower densities. This can be explained by observing that as U_R/U_A increases, the repulsive shoulder becomes less and less penetrable. So for U_R/U_A sufficiently large the fluid behaves as a fluid of hard spheres with radius equal to the external radius b of the shoulder. Consequently, the critical density tends to the value $\rho_c = \rho_{HS}/b^3$, where ρ_{HS} is the critical density for a fluid of hard spheres having radius 1.

Comparing figures 2 and 3 we note an important difference. For the case with the wider shoulder, as U_R/U_A increases the instability line becomes rather flat, instead of decreasing, at high densities. This suggests that a marked topological change might be observed for a potential with an even wider shoulder. So we next considered a potential with $b/a = 2$, $c/a = 2.2$. The results, shown in figure 4, show that for intermediate values of U_R/U_A the instability line has two clearly distinct maxima, thus suggesting the possible presence of two critical points in the phase diagram of the fluid. For large values of U_R/U_A, this feature disappears and the instability line becomes that typical of a fluid of hard spheres with radius b. Finally in figure 5 we show the results obtained for $b/a = 2.5$, $c/a = 3$. In this case also, we found an instability line with two maxima.

Having obtained, through the HNC equation, an estimate of the phase behaviour of the system, we choose a set of potential parameters ($b/a = 2.0$, $c/a = 2.2$ and $U_R/U_A = 0.5$) for which we expect the system to exhibit two critical points, and perform an accurate study of the phase diagram making use of MD simulation. We perform MD simulations in 3D at constant volume V and number of particles $N = 490$ and 850. We use periodic boundary conditions, a standard collision event list algorithm [19] and a modified Berendsen method to control T [24].

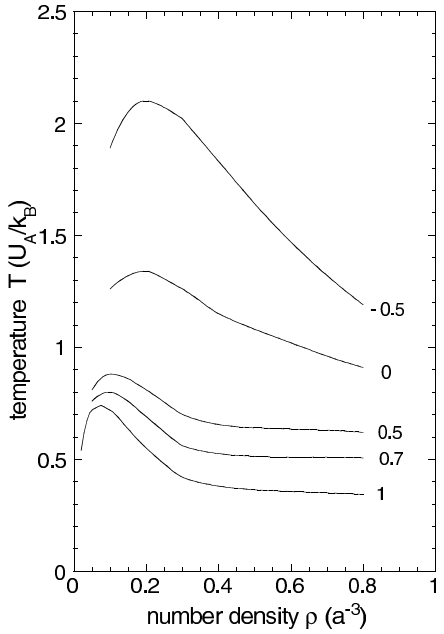

Figure 3. The instability line of the HNC equation ($b/a = 1.7$, $c/a = 2$). Each curve is labelled with the corresponding value of U_R/U_A.

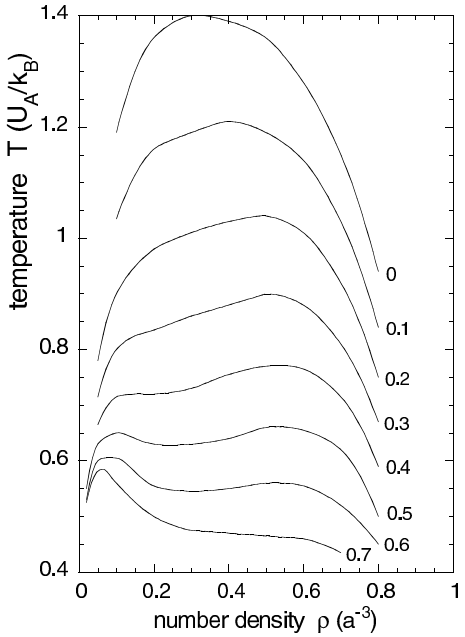

Figure 4. The instability line of the HNC equation ($b/a = 2$, $c/a = 2.2$). Each curve is labelled with the corresponding value of U_R/U_A.

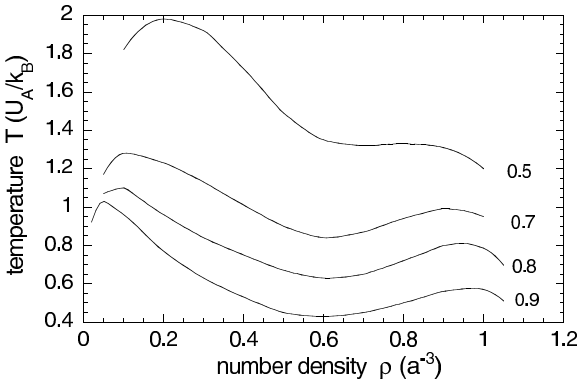

Figure 5. The instability line of the HNC equation ($b/a = 2.5$, $c/a = 3$). Each curve is labelled with the corresponding value of U_R/U_A.

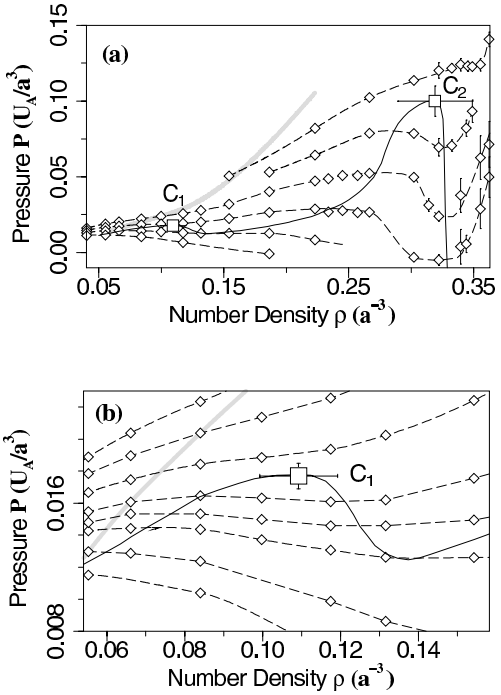

Figure 6. The pressure–density isotherms, crystallization line and spinodal line from the MD simulations. (*a*) Several isotherms for (bottom to top) $k_BT/U_A = 0.57$, 0.59, 0.61, 0.63, 0.65, 0.67 (k_B is the Boltzmann constant). Diamonds represent data points and lines are guides for the eyes. The solid line connecting local maxima and minima along the isotherms represents the spinodal line. The two maxima of the spinodal line (squares) represent the two critical points C_1 and C_2. To determine the crystallization line (grey line) we place a crystal seed, prepared at very low T, in contact with the fluid, and check, for each (T, ρ), whether the seed grows or melts after 10^6 MD steps. (*b*) An enlarged view of (*a*) around the gas–LDL critical point C_1 for $k_BT/U_A = 0.570$, 0.580, 0.590, 0.595, 0.600, 0.610, 0.620, 0.630.

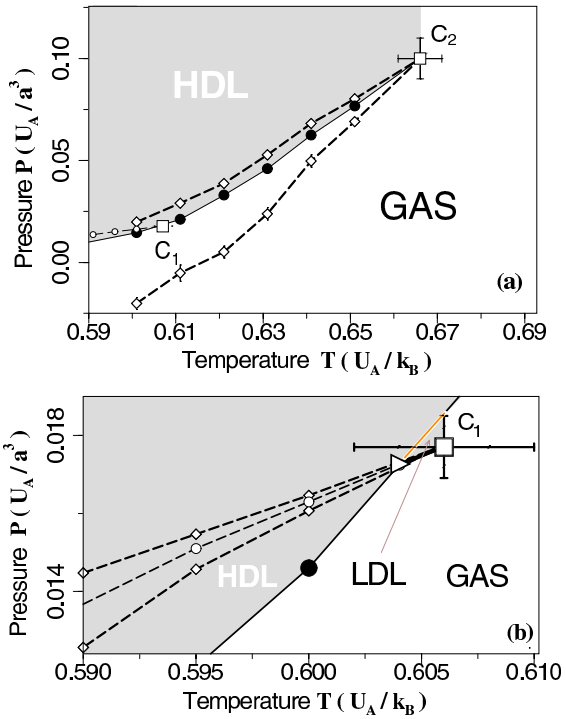

Figure 7. The P–T phase diagram, with coexistence lines and critical points resulting from MD simulations. (*a*) The solid black curve with dots is the gas–HDL coexistence line. The projection of the spinodal line is represented by diamonds with dashed lines. The critical point C_1 is for the gas–LDL transition, and C_2 is for the gas–HDL transition. (*b*) A blow-up of (*a*) in the vicinity of C_1. The gas–LDL coexistence line is represented by the solid curve in the stable portion (with respect to the HDL phase) and by the dashed curve with circles in the metastable region. The grey line is the LDL–HDL coexistence line. The triangle represents the triple point.

In our simulations we find two regions (figure 6) with negatively sloped isotherms and the overall shape of the spinodal line has two maxima, showing the presence of *two* critical points, C_1 and C_2. Using the Maxwell construction in the P–V plane [2], we evaluate the coexistence lines of the two fluid phases associated with each critical point (figure 7). Considering both the maxima of the spinodal line and the maxima of the coexistence regions in the P–ρ and P–T planes, we estimate the low-density critical point C_1 at $T_1 = 0.606 \pm 0.004\ U_A/k_B$, $P_1 = 0.0177 \pm 0.0008\ U_A/a^3$, $\rho_1 = 0.11 \pm 0.01\ a^{-3}$ and the high-density critical point C_2 at $T_2 = 0.665 \pm 0.005\ U_A/k_B$, $P_2 = 0.10 \pm 0.01\ U_A/a^3$, $\rho_2 = 0.32 \pm 0.03\ a^{-3}$. The critical point C_1 is at the end of the phase transition line separating the gas phase and the LDL phase, while the critical point C_2 is at the end of the phase transition line separating the gas phase and the HDL phase. Their relative positions resemble those in the phosphorus phase diagram, except that, in the experiments, C_2 has not been located [1]. The point where the gas–LDL coexistence line merges with the LDL–HDL coexistence line is a triple point where three fluid phases simultaneously coexist.

We considered also a different set of parameters ($b/a = 2.5$, $c/a = 3$ and $U_R/U_A = 0.8$) and calculated the phase diagram making use of a thermodynamically self-consistent integral theory (the so-called HMSA equation [25]). As shown in figure 8, the T–ρ phase diagram

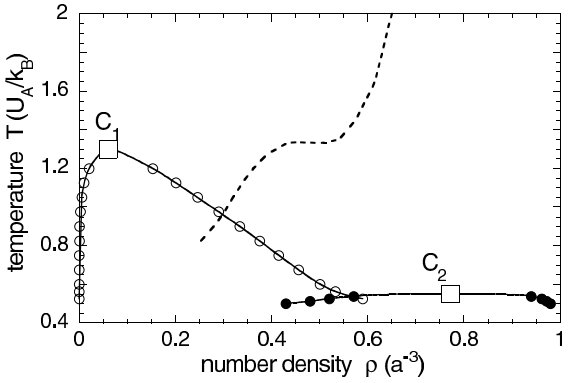

Figure 8. The T, ρ phase diagram obtained through the HMSA equation. Coexistence lines: gas–liquid (solid curve with circles), liquid–liquid (solid curve with dots). Squares represent the critical points. The dashed curve with no symbols is the freezing line estimated through the HV rule.

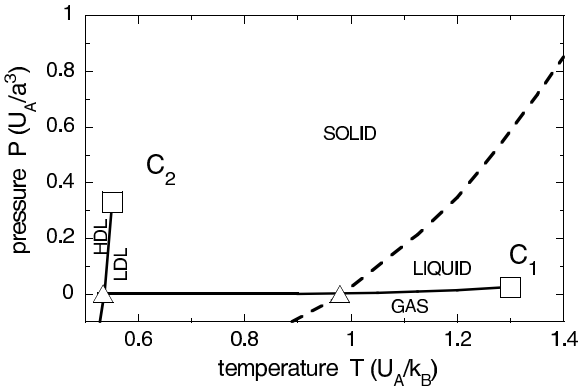

Figure 9. The P, T phase diagram obtained through the HMSA equation. Squares represent the critical points. Triangles represent the triple points. The dashed curve with no symbols is the freezing line estimated through the HV rule.

of the system exhibits two distinct binodal lines and thus two critical points, denoted as C_1 and C_2. The critical densities and temperatures are respectively $\rho_1 = 0.06$, $T_1 = 1.3$ and $\rho_2 = 0.77$, $T_2 = 0.55$. These values were estimated using the rectilinear diameter rule and the scaling relationship for the width of the coexistence curve with the non-classical exponent $\beta \approx 0.325$. Below T_1 the system separates into a gas and a liquid phase. Below T_2 the liquid phase separates into distinct LDL and HDL phases.

With respect to the case investigated through MD simulation, the relative position of the two critical points is inverted as far as the temperature is concerned, T_1 being, for the second set of parameters, higher than T_2. Moreover C_1 now lies in the stable region, while since the critical point C_2 is well below the freezing line (estimated using the Hansen–Verlet (HV) rule [21]), the liquid–liquid transition occurs between metastable phases in the supercooled region of the system. This feature resembles the scenario proposed for water [26, 27], but in that case the liquid–liquid coexistence line is expected to start from C_2, running at higher

pressures as T decreases [9]. In the system investigated, in contrast, this line runs at lower pressures as T decreases (see figure 9). Thus the gas–liquid and the liquid–liquid coexistence lines meet in a gas–liquid–liquid triple point which lies in the supercooled phase.

The results presented show that a pure model system, with a simple isotropic potential, may have a rich phase behaviour with features typical of substances characterized by complex anisotropic interactions. We note that the soft-core potential with the sets of parameters considered here displays no 'density anomaly' $(\partial V/\partial T)_P < 0$. This result is at first sight surprising, since soft-core potentials have often been used to explain the density anomaly (see, e.g., [2, 19]). The condition $(\partial V/\partial T)_P < 0$ implies $(\partial S/\partial V)_T < 0$, i.e. the disorder, measured by the entropy S, in the system increases for decreasing volume, as for water. This is consistent with the negative slope of the crystal–liquid transition line for water, as predicted by the Clausius–Clapeyron equation $\mathrm{d}P/\mathrm{d}T = \Delta S/\Delta V$, where ΔS and ΔV are the entropy and volume differences between the two coexisting phases. For our system we expect the reverse: $(\partial V/\partial T)_P > 0$ so $(\partial S/\partial V)_T > 0$, consistent with the positive slope of the LDL–HDL transition line $\mathrm{d}P/\mathrm{d}T$ (see figures 7 and 9).

According to our results, the presence of two critical points and the occurrence of the density anomaly are not necessarily related. Thus liquid–liquid phase transition may occur in systems with no density anomaly and in particular in liquid metals that can be described by soft-core potentials.

References

[1] Katayama Y, Mizutani T, Utsumi W, Shimomura O, Yamakata M and Funakoshi K 2000 *Nature* **403** 170
[2] Debenedetti P G 1998 *Metastable Liquids: Concepts and Principles* (Princeton, NJ: Princeton University Press)
[3] Brazhkin V V, Gromnitskaya E L, Stalgorova O V and Lyapin A G 1998 *Rev. High Pressure Sci. Technol.* **7** 1129
[4] Mishima O 2000 *Phys. Rev. Lett.* **85** 334
[5] Bellissent-Funel M-C 1998 *Nuovo Cimento* D **20** 2107
[6] Soper A K and Ricci M A 2000 *Phys. Rev. Lett.* **84** 2881
[7] Lacks D J 2000 *Phys. Rev. Lett.* **84** 4629
[8] van Thiel M and Ree F H 1993 *Phys. Rev.* B **48** 3591
[9] Poole P H, Sciortino F, Essmann U and Stanley H E 1992 *Nature* **360** 324
[10] Glosli J N and Ree F H 1999 *Phys. Rev. Lett.* **82** 4659
[11] Saika-Voivod I, Sciortino F and Poole P H 2001 *Nature* 412514
[12] Brazhkin V V, Popova S V and Voloshin R N 1997 *High Pressure Res.* **15** 267
[13] Franzese G, Malescio G, Skibinsky A, Buldyrev S and Stanley H E 2001 *Nature* **409** 692
[14] Malescio G and Pellicane G 2001 *Phys. Rev.* E **63** R020501
[15] Mon K K, Ashcroft M W and Chester G V 1979 *Phys. Rev.* B **19** 5103
[16] Stell G and Hemmer P C 1972 *J. Chem. Phys.* **56** 4274
[17] Kincaid J M and Stell G 1978 *Phys. Lett.* A **65** 131
[18] Debenedetti P G, Raghavan V S and Borick S S 1991 *J. Phys.: Condens. Matter* **95** 4540
[19] Sadr-Lahijany M R, Scala A, Buldyrev S V and Stanley H E 1998 *Phys. Rev. Lett.* **81** 4895
[20] Jagla E A 1999 *J. Chem. Phys.* **111** 8980
[21] Hansen J P and McDonald I R 1976 *Theory of Simple Liquids* (London: Academic)
[22] Poll P D and Ashcroft N W 1987 *Phys. Rev.* A **35** 5167
[23] Caccamo C 1996 *Phys. Rev.* **274** 1
[24] Berendsen H J C, Postma J P M, van Gunsteren W F, DiNola A and Haak J R 1984 *J. Chem. Phys.* **81** 3684
[25] Zerah G and Hansen J-P 1986 *J. Chem. Phys.* **84** 2336
[26] Mishima O and Stanley H E 1998 *Nature* **396** 329
Mishima O and Stanley H E 1998 *Nature* **392** 164
[27] Poole P H, Sciortino F, Grande T, Stanley H E and Angell C A 1994 *Phys. Rev. Lett.* **73** 1632